

# Effective equation of state in modified gravity and observational constraints

Simran Arora<sup>1,\*</sup>, Xin-he Meng<sup>2,†</sup>, S. K. J. Pacif<sup>3,‡</sup> and P.K. Sahoo<sup>1,§</sup>

<sup>1</sup>*Department of Mathematics, Birla Institute of Technology and Science-Pilani,  
Hyderabad Campus, Hyderabad-500078, India.*

<sup>2</sup>*School of Physics, Nankai Univ, P.R. China.*

<sup>3</sup>*Department of Mathematics, School of Advanced Sciences,  
Vellore Institute of Technology, Vellore 632014, Tamil Nadu, India.*

(Dated: July 16, 2020)

In this article, the bulk viscosity is introduced in a modified gravity model. The gravitational action has a general  $f(R, T)$  form, where  $R$  and  $T$  are the curvature scalar and the trace of energy momentum tensor respectively. An effective equation of state (EoS) has been investigated in the cosmological evolution with bulk viscosity. In the present scenario, the Hubble parameter which has a scaling relation with the redshift can be obtained generically. The role of deceleration parameter  $q$  and equation of state parameter  $\omega$  is discussed to explain the late-time accelerating expansion of the universe. The statefinder parameters and Om diagnostic analysis are discussed for our obtained model to distinguish from other dark energy models together with the analysis of energy conditions and velocity of sound for the model. We have also numerically investigated the model by detailed maximum likelihood analysis of 580 Type Ia supernovae from Union 2.1 compilation datasets and updated 57 Hubble datasets (31 data points from differential age method and 26 points from BAO and other methods). It is with efforts found that the present model is in good agreement with observations.

PACS numbers: 95.36.+x, 04.50.kd, 98.80.Jk.

## I. INTRODUCTION

We still believe in that the Einstein's general theory of relativity (GR) does not give the final word to all gravity phenomena, though in the solar system tests GR is very successful so far. As well understood that after many observational and experimental tests, there are some issues which hint towards a possible modification to general theory of relativity (GR) at large scales such as the cosmic accelerating expansion phenomena and dark matter mysteries. The recently developed late time accelerated expansion [1–3] of the Universe is an immediate motivation for the same. The simplest possible modification for such an acceleration is to consider a cosmological constant  $\Lambda$  existence which plays the role of dark energy, i.e. the fluid responsible for an effective negative pressure. Another way to identify the role of dark energy is to treat it as an effective geometrical quantity coming out of a modified Einstein-Hilbert action. We can do this by replacing the Ricci curvature  $R$  in the Einstein action by a generic function  $f(R)$  which gives rise to the named  $f(R)$  theories as mentioned in [4–7], for example.

Several studies have been carried out on the modified

theories of gravity which can explain both early and late time expansion of the universe. The  $f(G)$  gravity form, for example, is also an important modified theory of gravity in which there is replacement of  $R$  by a general function  $f(G)$ , where  $G$  is the Gauss-Bonnet invariant [8, 9]. Other modified theories of gravity including  $f(T)$  form where  $T$  is the torsion,  $f(R, G)$ , and also  $f(R, T)$  forms, etc. without by direct introducing an effective dark energy term (cosmological constant like), can also give a satisfying explanation to present cosmic acceleration expansion. Some related works on these theories have been described in refs. [10–15].

**Viscosity:** In order to portray the recent accelerated expansion era, the framework of GR and so called cosmological constant  $\Lambda$ CDM model with vacuum and dust energy is not sufficient as it is faced with some shortcomings. The two main issues are the coincidence puzzle and the fine tuning problem. Though the evolutions of dark matter and dark energy are different, they are faced with the coincidence densities. On the other hand the fine tuning problem is associated with the disparity between the theoretical and the observational value of the cosmological constant. These problems have provoked the deliberations of various dark energy models like quintessence, perfect fluid models, scalar fields. Apart from these many authors have stated that the cosmic viscosity directs the late time acceleration expansion. The viscosity theories in cosmology is important when connected with the early universe,

\*Electronic address: [dawrasimran27@gmail.com](mailto:dawrasimran27@gmail.com)

†Electronic address: [xhm@nankai.edu.cn](mailto:xhm@nankai.edu.cn)

‡Electronic address: [shibesh.math@gmail.com](mailto:shibesh.math@gmail.com)

§Electronic address: [pkshoo@hyderabad.bits-pilani.ac.in](mailto:pkshoo@hyderabad.bits-pilani.ac.in)

i.e. when the temperature was about  $10^4\text{K}$  (at the time of neutrino parting). There are two different viscosity coefficients in cosmic fluid namely bulk viscosity  $\zeta$  and shear viscosity  $\eta$ . We omit shear viscosity due to the accepted spatial isotropy of the universe like the Robertson-Walker metric descriptions.

By considering a bulk viscous fluid the problem of finding a viable mechanism for the origin of bulk viscosity in the expanding universe arises. Theoretically, bulk viscosity exists due to the deviations from the local thermodynamic irreversibility of the motion. In cosmology, bulk viscosity arises as an effective pressure to restore the system back into its thermal equilibrium [17]. Eckart [16] made the first approach for describing non-equilibrium thermodynamic effects in a relativistic context. It has also been studied that the bulk viscosity is sufficient to drive the cosmic fluid from the quintessence to phantom region [18]. Sharif and Yousaf [19] have also investigated into stability regions for a non-static restricted class of axially symmetric geometry. The work includes shearing viscous fluid that collapse non-adiabatically.

**Viscosity in modified gravity:** There have been a great variety of models describing the universe with dark energy discussed above. But if we talk about the problem of cosmic adaptation, i.e. the mean stage of low redshift, the cosmic accelerating expansion can be justified by the approach of modification in Einstein equations geometrically. Bulk viscosity can also produce an acceleration without the need of scalar field or cosmological constant if connected to inflation. The bulk viscosity contributes to the pressure term and exerts extra pressure driving the accelerating expansion of the universe [20]. Also, the effective negative pressure due to the viscous media effects the key condition to generate inflation.

Most of the time argument on standard gravity assume the cosmic fluid to be ideal that is non-viscous. If we see from hydrodynamics point of view, two viscosity coefficients discussed above come into play which means deviation from thermal equilibrium to the first order. This theory is an acceptance of Eckart 1940 theory. The important part of this is the non-casual behavior. Therefore taking second order deviations from a thermal equilibrium leads to a casual theory respecting special relativity. Now, it is also important to take into account some more realistic models, which process due to complicated viscosity, as that Singh and Kumar [21] have studied the role of bulk viscosity in the evolution of the Universe by considering the modified  $f(R, T)$  gravity model. There were remarkable cosmological applications of viscous imperfect fluids in 1970s [22, 23]. Also

many other authors have investigated the idea of bulk viscous fluids to explain the acceleration of the Universe expansion [18, 24–27]. Davood [28] also studied the role of bulk viscosity in  $f(T)$  gravity. The cosmic pressure in this phenomenon is considered as  $p = (\gamma - 1)\rho - 3\zeta H$ , where the  $\gamma$  parameterizes the EoS [29]. The form of this pressure was originally proposed by Eckart [16]. However, Eckart theory undergoes some anatomies. One of those is the instability of the equilibrium states [30]. Another is that the dissipative perturbations propagate at infinite speeds [31]. In 1979, a more general theory was developed by Israel and Stewart [32] which was casual and stable. Eckart theory can also be obtained in the first order limit in Stewart theory when the relaxation time tends to zero. So, if we talk about the limiting case, Eckart theory is a good approximation which is also discussed in [33]. Hence, we know that Eckart theory is less complicated than the Israel-Stewart theory irrespective of drawbacks it have. Many authors have also pointed out that, the relaxation time is to be constant in Israel-Stewart theory which is not reasonably correct in expanding universe.

From the observational constraints, we have that the current EoS parameter  $\omega = \frac{p}{\rho}$  is around  $-1$  [34, 35], probably larger than  $-1$  by the recent DES results, which is called the quintessence range while the EoS below  $-1$  corresponding to the so called phantom region. In this article we have observed that the focused model we have investigated into shows accelerating behavior and behaves as the quintessence alike ( $\omega > -1$ ) as current datasets favored.

Fisher and Carlson [36] have examined the form of  $f(R, T) = f_1(R) + f_2(T)$ , in which they state that  $f(R, T)$  yields a new physics and limits could be placed on the cross-terms by comparison with observations. This work is again reexamined by Harko and Moreas [37] in examining observational restrictions on the function  $f_2(T)$ . Setare and Houndjo [38] have studied the finite-time future singularities model in  $f(T)$  gravity with the effect of viscosity. Sharif and Rani [39] have also worked on viscous dark energy in  $f(T)$  gravity. The work of Iver Brevik [40] describes viscosity in  $f(R)$  gravity.

In the present article, we study the Friedman-Lemaitre-Robertson-Walker (FLRW) geometric frame model with bulk viscosity effects in the modified  $f(R, T)$  gravity theory, in which we have investigated into a general effective equation of state form given by,

$$p = (\gamma - 1)\rho + p_0 + \omega_H H + \omega_{H^2} H^2 + \omega_{dH} \dot{H},$$

and also shown that the following time-dependent bulk viscosity

$$\zeta = \zeta_0 + \zeta_1 H + \zeta_2 \left(\frac{\dot{H}}{H} + H\right)$$

is the same form as derived by the above mentioned ef-

fective EoS. The field equations and its exact solutions are obtained with constant  $\alpha$  by assuming the model simplest form of  $f(R, T) = R + 2f(T)$  where  $f(T) = \alpha T$ . This is the simplest functional choice of  $f(R, T)$  gravity as when  $\alpha = 0$ , the field equations correspond to that of GR ones.

The article has been discussed in various sections as follows. In section II, we have formulated the field equations followed by modeling with viscosity. We have described the general solution and the behavior of various parameters in section III. In Sec IV we have performed various tests to check the validation of model containing the energy conditions, velocity of sound, statefinder parameter, the Om diagnostics and also observational datasets corresponding to SNeIa and  $H(z)$ . And the last section V is followed by the conclusion. We have taken the Einstein field equations in units of  $8\pi G = c = 1$ .

## II. FIELD EQUATIONS

The  $f(R, T)$  theory is a modified theory of gravity in which the most general action for  $f(R, T)$  gravity is given as in Ref. [12, 21]

$$S = \frac{1}{2} \int d^4x \sqrt{-g} (f(R, T) + 2L_m), \quad (1)$$

where the Einstein-Hilbert Lagrangian,  $R$ , has been replaced by an arbitrary function of the Ricci scalar curvature  $R$  and the trace  $T$  of the energy momentum tensor. Here,  $g$  is the determinant of the metric tensor  $g_{\mu\nu}$  and  $L_m$  is the matter Lagrangian density.

Variation of the action with respect to the metric tensor gives us the following gravitational field equation:

$$f_R(R, T)R_{\mu\nu} - \frac{1}{2}f(R, T)g_{\mu\nu} + (g_{\mu\nu}\square - \nabla_\mu\nabla_\nu)f(R, T) = T_{\mu\nu} - f_T(R, T)T_{\mu\nu} - f_T(R, T)\Theta_{\mu\nu}, \quad (2)$$

where,  $\nabla_\mu$  and  $\nabla_\nu$  represents the covariant derivative and  $\Theta_{\mu\nu}$  is defined by

$$\Theta_{\mu\nu} \equiv g^{\alpha\beta} \frac{\delta T_{\alpha\beta}}{\delta g^{\mu\nu}}. \quad (3)$$

We consider the Friedman-Lemaitre-Robertson-Walker (FLRW) metric in the flat space geometry ( $k = 0$ )

$$ds^2 = dt^2 - a^2(t)[dr^2 + r^2d\theta^2 + r^2\sin^2\theta d\phi^2] \quad (4)$$

where  $a(t)$  is the cosmic scale factor.

The components of four-velocity  $u^\mu$  are  $u^\mu = (1, 0)$  in comoving coordinates. Assume that the cosmic fluid possesses a bulk viscosity  $\zeta$ . We have the energy-momentum tensor for a viscous fluid as follows

$$T_{\mu\nu} = \rho u_\mu u_\nu - \bar{p}h_{\mu\nu}. \quad (5)$$

where  $h_{\mu\nu} = g_{\mu\nu} + u_\mu u_\nu$  and  $\bar{p} = p - 3\zeta H$  is the effective pressure.

If we choose the Lagrangian density as  $L_m = -\bar{p}$  then the tensor  $\Theta_{\mu\nu}$  becomes

$$\Theta_{\mu\nu} = -2T_{\mu\nu} - \bar{p}g_{\mu\nu}. \quad (6)$$

Using (5) and (6), the field equation for the bulk viscous fluid become

$$R_{\mu\nu} - \frac{1}{2}Rg_{\mu\nu} = T_{\mu\nu} + 2f'(T)T_{\mu\nu} + (2\bar{p}f'(T) + f(T))g_{\mu\nu}. \quad (7)$$

For the particular choice of the function  $f(T) = \alpha T$ , where  $\alpha$  is a constant, we get field equations as

$$3H^2 = \rho + 2\alpha(\rho + \bar{p}) + \alpha T, \quad (8)$$

$$2\dot{H} + 3H^2 = -\bar{p} + \alpha T, \quad (9)$$

where  $T = \rho - 3\bar{p}$ . From Eqs. (8) and (9), we have

$$2\dot{H} + (1 + 2\alpha)(\rho + \bar{p}) - 3(1 + 2\alpha)\zeta H = 0. \quad (10)$$

## III. GENERAL SOLUTION

We can see the Eqs. (8) and (9) contains four unknown parameters viz.  $\rho, p, \zeta$  &  $H$ . To get an exact solution, we need two more physically viable equations. As discussed in the introduction, we shall consider the following EoS (an explicit form as given in [29])

$$p = (\gamma - 1)\rho + p_0 + \omega_H H + \omega_{H2} H^2 + \omega_{dH} \dot{H}, \quad (11)$$

where  $p_0, \omega_H, \omega_{H2}, \omega_{dH}$  are free parameters. If we compare with the bulk viscosity form we get the most general one. We show that this time-dependent bulk viscosity

$$\zeta = \zeta_0 + \zeta_1 \frac{\dot{a}}{a} + \zeta_2 \frac{\ddot{a}}{a}, \quad (12)$$

is effectively equivalent to the form derived by using Eq. (11) where  $\zeta_0, \zeta_1, \zeta_2$  are constants.

The reason behind this is

$$\begin{aligned} \bar{p} &= p - 3\zeta H = p - 3(\zeta_0 + \zeta_1 \frac{\dot{a}}{a} + \zeta_2 \frac{\ddot{a}}{a})H \\ &= p - 3\zeta_0 H - 3\zeta_1 H^2 - 3\zeta_2 (\dot{H} + H^2) \end{aligned}$$

which gives

$$\bar{p} = p - 3\zeta_0 H - 3(\zeta_1 + \zeta_2)H^2 - 3\zeta_2 \dot{H}. \quad (13)$$

We can obtain the corresponding coefficients are

$$\begin{aligned} \omega_H &= -3\zeta_0, \\ \omega_{H2} &= -3(\zeta_1 + \zeta_2), \\ \omega_{dH} &= -3\zeta_2. \end{aligned}$$

Using Eqs. (8), (11), (12), (13), we obtain the explicit form of energy density as

$$\rho = \frac{\alpha p_0 + 2\alpha\omega_H H + (2\alpha\omega_{H2} + 3)H^2 + 2\alpha\omega_{dH}\dot{H}}{1 + 4\alpha - \alpha\gamma}. \quad (14)$$

Subsequently, using Eq.(9) we obtain the bulk viscous pressure as

$$\bar{p} = \frac{\alpha^2 p_0 + 2\alpha^2 \omega_H H + (2\alpha^2 \omega_{H2} - 9\alpha - 3 + 3\alpha\gamma)H^2 + (2\alpha^2 \omega_{dH} - 2(1 + 4\alpha - \alpha\gamma))\dot{H}}{(1 + 4\alpha - \alpha\gamma)(1 + 3\alpha)}. \quad (15)$$

Using Eqs. (10), (11), (14), we have an equation

$$\left[ 2 + \frac{2(1+2\alpha)\omega_{dH}(1+4\alpha)}{1+4\alpha-\alpha\gamma} \right] \dot{H} + \left[ \frac{2(1+2\alpha)\omega_H(1+4\alpha)}{1+4\alpha-\alpha\gamma} \right] H + \left[ \frac{(1+2\alpha)(2\omega_{H2}(1+4\alpha)+3\gamma)}{1+4\alpha-\alpha\gamma} \right] H^2 + \left[ \frac{(1+2\alpha)p_0(1+4\alpha)}{1+4\alpha-\alpha\gamma} \right] = 0. \quad (16)$$

Because of the high non linearity, it is difficult to solve the above equation (16) for which without the loss of generality we assume that  $p_0 = 0$ . This simplifies the equation to give the time evolution of Hubble parameter  $H$  as,

$$H = \frac{k_1}{k_3 e^{k_1 t} - k_2}, \quad (17)$$

where  $k_1 = \frac{2(1+2\alpha)\omega_H(1+4\alpha)}{1+4\alpha-\alpha\gamma}$ ,  $k_2 = \frac{2(1+2\alpha)\omega_{dH}(1+4\alpha)}{1+4\alpha-\alpha\gamma}$  and  $k_3 = \frac{(1+2\alpha)(2\omega_{H2}(1+4\alpha)+3\gamma)}{1+4\alpha-\alpha\gamma}$  and  $k_3 = k_1 c_1$ , with  $c_1$  being a constant of integration.

Using the definition  $H = \frac{\dot{a}}{a}$ , we can obtain the scale factor given by,

$$a = k_4 k_3^{-\frac{1}{k_2}} (k_3 - k_2 e^{-k_1 t})^{\frac{1}{k_2}}, \quad (18)$$

where  $k_4$  is a constant of integration.

Finally, the deceleration parameter ( $q = -\frac{\ddot{a}a}{\dot{a}^2}$ ) is obtained as,

$$q = -1 + k_3 e^{k_1 t}. \quad (19)$$

Now, we have the general set of solution for the formulated system. In order to discuss the detailed evolution of the Universe in various phases, we shall discuss the

behavior of the different cosmological parameters obtained here. In the present article, we are interested to examine the different regimes of the Universe particularly the phase transition from decelerated to accelerated by constraining the model parameters. We know a positive value of  $q$  refers the decelerating phase while a negative value of  $q$  corresponds to accelerating phase of the universe. So, we shall write all the cosmological parameters in terms of redshift  $z$  using the relation

$$a(t) = \frac{1}{1+z} \quad (20)$$

with  $a_0 = 1$ . The Hubble parameter and the deceleration parameter are two observable parameters which can be rewritten in terms of redshift as,

$$H(z) = \frac{k_1}{k_2} ((k_4 + k_4 z)^{k_2} - 1), \quad (21)$$

and

$$q(z) = -1 + k_2 \frac{(k_4 + k_4 z)^{k_2}}{(k_4 + k_4 z)^{k_2} - 1}. \quad (22)$$

Recent studies reveals that the present observed deceleration rate of the Universe is  $q_0 = -0.51_{-0.01}^{+0.09}$  [41] and a transition redshift from deceleration to acceleration is  $z_t = 0.65_{-0.17}^{+0.19}$  [42]. In literature [43–45] reported that the Universe passed from a decelerated phase to an accelerated one at  $z_t \approx 0.7$  [46]. So, we have chosen the values of these free parameters ( $k_1, k_2, k_3, k_4$ ) in the present

model in such way that our  $q_0$  and  $z_t$  result are consistent with values reported in the literature. Henceforth, we will discuss a particular model as an exemplification and study the cosmic history of the universe with some numerical choice of the values of the model parameters. However, we have chosen the values of  $k_2$  and  $k_4$  that has been constrained from some observational datasets in the subsequent section. The evolution of  $q(z)$  is shown in the following Fig. 1 with suitable choice of the model parameters.

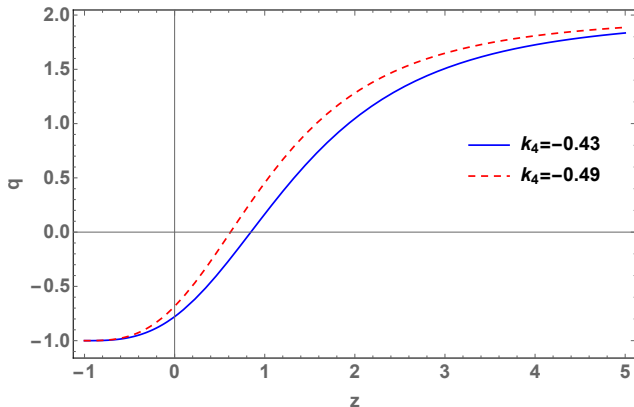


FIG. 1: The plot discusses the behavior of deceleration parameter versus redshift  $z$  for the model with  $k_2 = 3$  and  $k_4 = -0.43, -0.49$ .

From Fig. 1, we see that the deceleration parameter  $q$  varies from negative to positive at  $z_t = 0.845815$  and  $z_t = 0.619797$  with  $q_0 = -0.779046$  and  $q_0 = -0.684206$  with two different values of  $k_4 = -0.43$  and  $k_4 = -0.49$  respectively. This indicates, the universe exhibits a transition from early deceleration to the current acceleration in this model. The behavior of  $\rho$  and  $\bar{p}$  from equations (14) and (15) with respect to redshift  $z$  is plotted below.

Since we have constrained the values of  $k_2$  and  $k_4$  in section IV F, so accordingly the values of other model parameters such as  $\alpha, \gamma, \omega_H, \omega_{H2}, \omega_{dH}$  involved in  $k_1, k_2$  and  $k_3$  are set for the analysis. We can clearly observe the behavior of  $\rho$  and  $\bar{p}$  from the Figs. 2 & 3, which shows that energy density is an increasing function of  $z$  and the effective pressure has a transition from negative to positive. The present study demonstrate the expanding behavior of the universe and on the other hand negative pressure indicates the cosmic accelerated expansion of the universe.

The EoS parameter is the relationship between pressure  $p$  and energy density  $\rho$ . The EoS parameter is used to classify the decelerated and accelerated expansion of the universe and it categorizes various epochs as follows: when  $\omega = 1$ , it represents stiff fluid, if  $\omega = 1/3$ ,

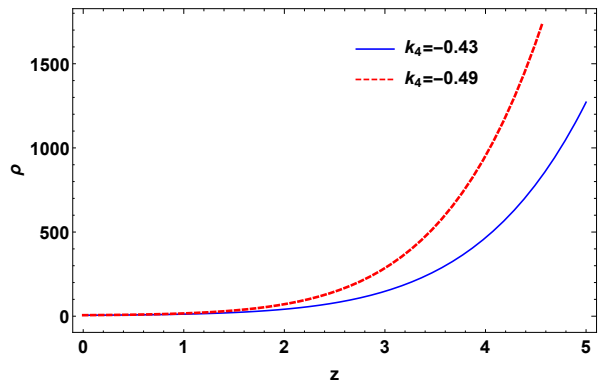


FIG. 2: The plot shows the behavior of density parameter of the model versus redshift  $z$  with  $\alpha = -0.1, \gamma = 1.01, \omega_H = 4.1, \omega_{H2} = 1.57, \omega_{dH} = -0.1$  and  $k_4 = -0.43, -0.49$ .

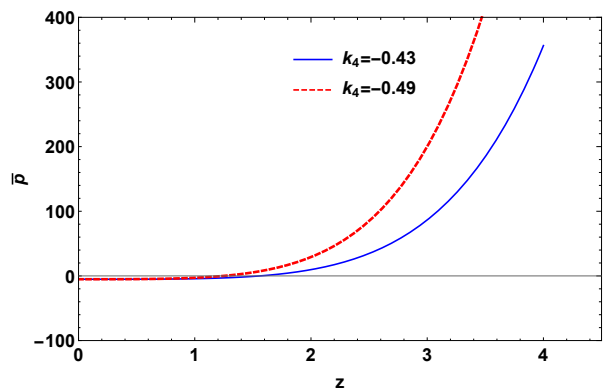


FIG. 3: The plot shows the behavior of effective pressure of the model versus redshift  $z$  with  $\alpha = -0.1, \gamma = 1.01, \omega_H = 4.1, \omega_{H2} = 1.57, \omega_{dH} = -0.1$  and  $k_4 = -0.43, -0.49$ .

the model shows the radiation dominated phase while  $\omega = 0$  represents matter dominated phase. In the present accelerated phase of evolution,  $0 \geq \omega > -1$  shows the quintessence phase and  $\omega = -1$  shows the cosmological constant, i.e.,  $\Lambda$ CDM model and  $\omega < -1$  yields the phantom era. In Fig. 4, we have plotted the EoS parameter versus redshift  $z$  by considering same values of the model parameters as discussed above,

The graph in Fig. 4 shows that the as  $z \rightarrow -1, \omega \rightarrow -1$  in the future. It also shows the transition from negative to positive in due course of evolution which indicates the earlier decelerating phase of the universe with positive pressure (suitable for structure formation) and present accelerating phase of the evolution with negative pressure. The present values of the EoS parameter can be calculated as of  $\omega_0 = -0.888046$  for  $k_4 = -0.43$  and  $\omega_0 = -0.838394$  for  $k_4 = -0.49$  together with other stated values of other model parameters. In the following section we discuss the of the obtained model with



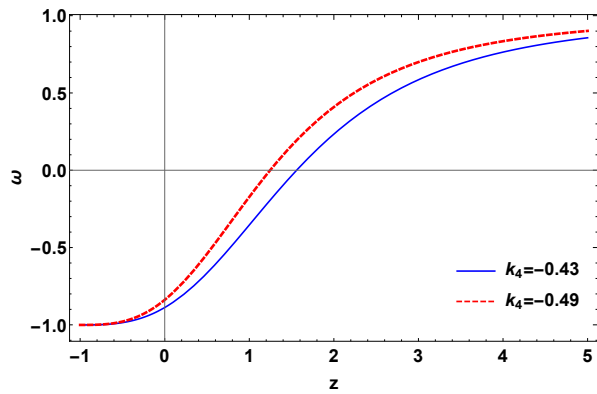


FIG. 4: The plot shows the behavior of Equation of State of the model versus redshift  $z$  with  $\alpha = -0.1$ ,  $\gamma = 1.01$ ,  $\omega_H = 4.1$ ,  $\omega_{H2} = 1.57$ ,  $\omega_{dH} = -0.1$ ,  $k_4 = -0.43, -0.49$ .

some mathematical tools and observational datasets.

#### IV. TESTS FOR VALIDATION OF THE MODEL

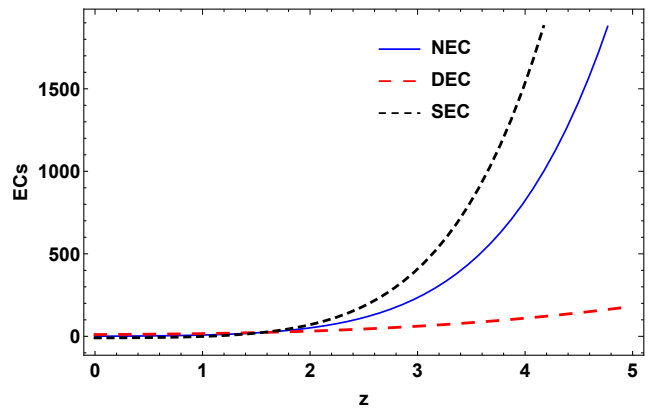
There are some theoretical and observational tests to check the validity of any cosmological model. So now, we shall discuss some of the cosmological tests for the validation of our obtained model.

##### A. Energy conditions

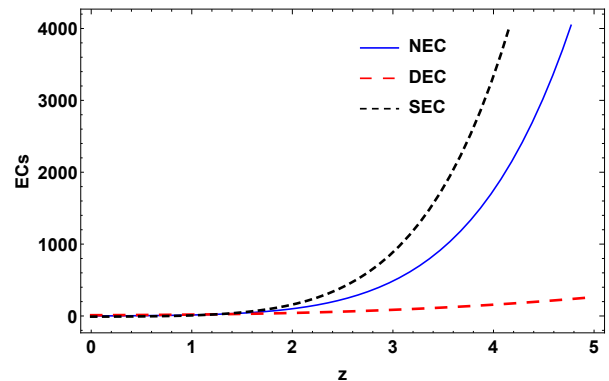
The energy conditions (ECs) of GR permit one to deduce very powerful and general theorems about the behavior of strong gravitational fields and cosmological geometries [47]. ECs have a great adequacy in classical GR which consider the singularity problems of space-time and explain the behavior of null, space-like, time-like or light-like geodesics. It provides us some flexibility to analyze certain ideas about the nature of cosmological geometries and some relations that the stress energy momentum must satisfy to make energy density positive. It is normally used in GR to show and study the singularities of space-time [48]. In general, ECs can be classified as a) SEC (Strong energy condition), b) DEC (Dominant energy condition), c) WEC (Weak energy condition) and d) NEC (Null energy condition) [49]. The formulation of these four types of ECs in GR is expressed as:

a) SEC: Gravity should always be attractive and in cosmology  $\rho + 3p \geq 0$ .

b) DEC: The matter energy density measured by any observer must be positive and propagate in a causal way, which leads to  $\rho \geq |p|$ .



a) with  $k_4 = -0.43$



b) with  $k_4 = -0.49$

FIG. 5: Behavior of Energy conditions of the model versus redshift  $z$  with  $\alpha = -0.1$ ,  $\gamma = 1.01$ ,  $\omega_H = 4.1$ ,  $\omega_{H2} = 1.57$ ,  $\omega_{dH} = -0.1$  and  $k_4$  as mentioned in (a) & (b).

c) WEC: The matter energy density measured by any observer should be positive,  $\rho \geq 0$ ,  $\rho + p \geq 0$ .

d) NEC: It's the minimum requirement that is implied by SEC and WEC, is  $\rho + p \geq 0$ .

The violation of NEC implies that none of the mentioned ECs are validated. The SEC is currently the subject of much discussion for the current accelerated expansion of the Universe [50, 51]. SEC must be violated in cosmological scenarios during the inflationary expansion and at the present time [52].

The graph of the energy conditions is given below.

We examine that NEC, DEC hold but SEC violates the model which directly implies the accelerated expansion of the Universe.

##### B. Velocity of sound

The velocity of sound plays a similar role to that of equation of state for the background cosmology, which

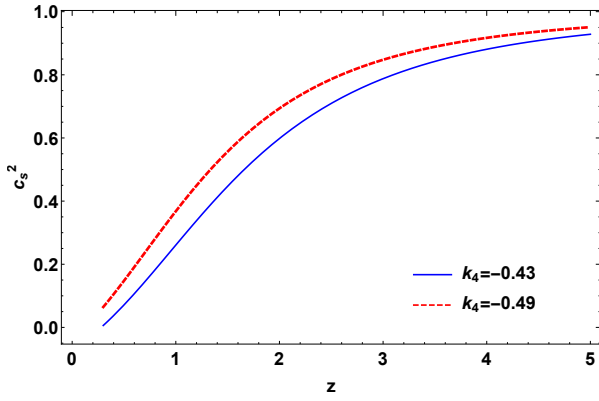


FIG. 6: Velocity of sound  $c_s^2$  vs redshift  $z$ .

relates the pressure and density as in [53],

$$c_s^2 = \frac{dp}{d\rho}$$

In this study, we have taken speed of light  $c$  to be 1, so the stability condition for the model is  $0 \leq c_s^2 \leq 1$ . The lower bound prevents dark energy fluctuations from growing exponentially, which can lead to non-physical situations and the upper one is imposed in order to avoid super-luminal propagation. Guillermo and Julien [54] reviewed the concept of sound speed for a cosmo-

logical fluid. The non trivial issue of initial conditions for dark energy perturbations in the radiation era is studied which is a priori non-adiabatic since  $c_s^2 > \omega$ . The square of the sound speed for bulk viscosity in GR is presented in [29].

According to the graph above it can be seen that the model satisfies  $c_s^2 \leq 1$  throughout. Therefore, we can say that our model is stable.

### C. Statefinder diagnostics

In [55], Sahni et al. have introduced a new cosmological diagnostic pair  $\{r, s\}$  - Statefinder. The parameters  $r$  and  $s$  are dimensionless and are constructed from the scale factor  $a(t)$  and its time derivatives similar to the geometrical parameters  $H(z)$  and  $q(z)$ . The Statefinder help to differentiate and compare between different dark energy models. The standard cold dark model (SCDM) and the cosmological constant model ( $\Lambda$ CDM) have some fixed points in the  $s$ - $r$  plane and  $q$ - $r$  plane. Any obtained model can be compared with these standard ones to see how a model approaches or deviates from these models. The expressions  $r, s$  for our model are obtained as,

$$r = - \frac{\left(\frac{k_3^{1/k_2}}{k_4 z + k_4}\right)^{-3k_2} \left(\left(\frac{k_3^{1/k_2}}{k_4 z + k_4}\right)^{k_2} - k_3\right) \left(- (k_2 - 2)(k_2 - 1)k_3 \left(\frac{k_3^{1/k_2}}{k_4 z + k_4}\right)^{k_2} + \left(\frac{k_3^{1/k_2}}{k_4 z + k_4}\right)^{2k_2} + (k_2 - 1)(2k_2 - 1)k_3^2\right)}{\left((k_4(z+1))^{k_2} - 1\right)^3} \quad (23)$$

$$s = - \frac{\left(\left(\frac{k_3^{1/k_2}}{k_4 z + k_4}\right)^{k_2} - k_3\right) \left(- (k_2 - 2)(k_2 - 1)k_3 \left(\frac{k_3^{1/k_2}}{k_4 z + k_4}\right)^{k_2} + \left(\frac{k_3^{1/k_2}}{k_4 z + k_4}\right)^{2k_2} + (k_2 - 1)(2k_2 - 1)k_3^2\right) \left(\frac{k_3^{1/k_2}}{k_4 z + k_4}\right)^{-3k_2}}{\left((k_4(z+1))^{k_2} - 1\right)^3} + 1 \quad (24)$$

$$3 \left( \frac{k_2}{(k_4(z+1))^{k_2} - 1} + k_2 - 1.5 \right)$$

Although, the presented model do not contain any extra source term (dark energy) but the bulk viscous term exerts extra pressure and plays the role of the dark energy. The following are plots show the behavior of our obtained model compared with the SCDM and  $\Lambda$ CDM models.

In the Fig.7, the model behavior is shown in  $s$ - $r$  plane which is somewhat similar to [33]. The point  $(s, r) =$

$(0, 1)$  corresponds to the  $\Lambda$ CDM of the universe. Our model is also resembling to the  $\Lambda$ CDM in future and ultimately freezing to it. Similarly, Fig.8 shows that our model approaching to the de Sitter point ( $q = -1, r = 1$ ) and deviated from the SCDM model.

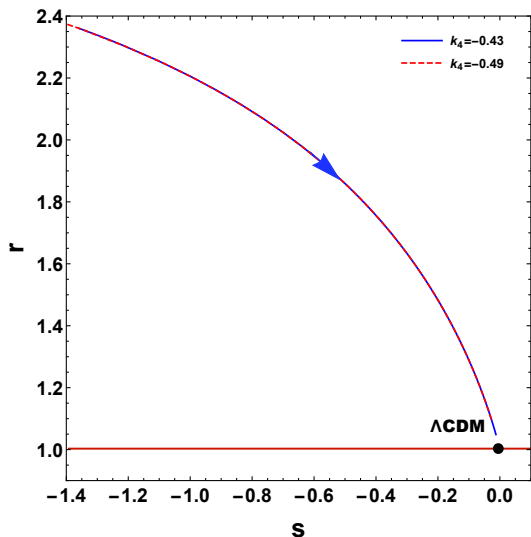


FIG. 7: The plot shows the behavior of the presented model in the  $s$ - $r$  plane and  $\Lambda$ CDM model.

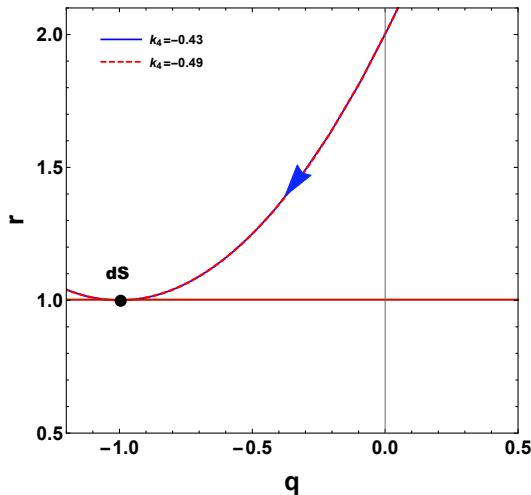


FIG. 8: The plot shows the behavior of the presented model in the  $q$ - $r$  plane  $\Lambda$ CDM model.

#### D. $Om$ diagnostic

Now, we turn to a discussion on  $Om$  diagnostic written as  $Om(z)$ .  $Om(z)$  is used to differentiate standard  $\Lambda$ CDM model from various dark energy models [56]. In the analysis of  $Om$  diagnostic only first order derivative are used as it involves the Hubble parameter depending on a single time derivative of  $a(t)$ . In reference with Sahni et al. [57] and Zunckel and Clarkson [58],  $Om(z)$  for flat universe is defined as

$$Om(z) = \frac{\left(\frac{H(z)}{H_0}\right)^2 - 1}{(1+z)^3 - 1} \quad (25)$$

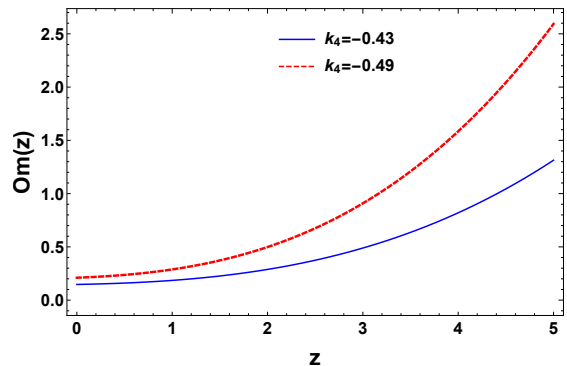


FIG. 9: Behavior of  $Om$  versus redshift  $z$

Thus, we have different values of  $Om(z)$  for the  $\Lambda$ CDM model, phantom and quintessence cosmological models. According to the curvature variation, we can describe the behavior of dark energy as quintessence type ( $\omega > -1$ ) corresponding to negative curvature, phantom type ( $\omega < -1$ ) corresponding to its positive curvature and  $Om(z)=\Lambda$ CDM to zero curvature. The parametrization of  $Om(z)$  is done in [59] to show how the combination of most recent and naturally improved observations about the  $H(z)$  and SNeIa be implemented to study the consistency or acknowledge the tension between the  $\Lambda$ CDM model and observations. The behavior can be easily seen in Fig. 9 which shows that at late times, the growth of  $Om(z)$  favors the decaying dark energy models as discussed in [60].

$$Om(z) = \frac{1 \cdot \left(\frac{(k_4 z + k_4)^{k_2} - 1}{k_4^{k_2} - 1}\right)^2 - 1}{(z+1)^3 - 1} \quad (26)$$

#### E. Fitting the model with $H(z)$ & SNIa datasets

Study of the structure, the origin and the evolution of the universe through observations is known as observational cosmology. Several types of observational datasets are available at present for different measurements such as Type Ia Supernovae [1, 2] data, Cosmic Microwave Background Radiation [35] data, Baryon Acoustic Oscillations [61] data, Planck data etc. and are some spectacular observations providing strong evidence for the acceleration of the universe. So, we shall check the viability of our obtained model with any of these datasets. Here, we have taken into account 57 points of  $H(z)$  data (Appendix Table 2.), wherein 31 points of Hubble data points are from the differential age method and 26 points are from BAO and other



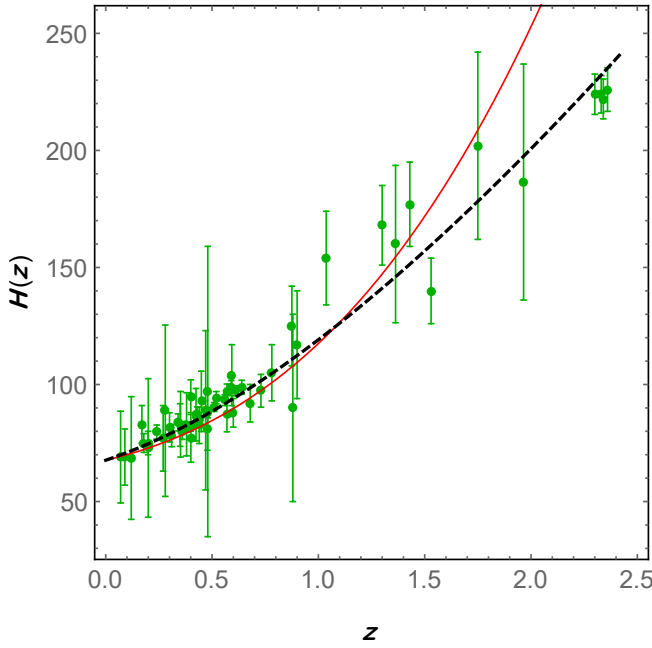


FIG. 10: The plot shows the 57 points of  $H(z)$  datasets (Blue dots) with corresponding error bars along with the presented model (solid red line) which has a better fit to the  $H(z)$  datasets for  $k_2 = 3$  and  $k_4 = -0.49$ .  $\Lambda$ CDM model is also shown in black dashed line for model comparison.

methods [62]. Secondly, we have taken into account 580 points of type Ia Supernovae from Union 2.1 compilation datasets [63, 64] to achieve our goal to find best fit values of the model parameters and compare to the  $\Lambda$ CDM model.

The  $\chi^2$  function for the  $H(z)$  datasets is taken to be

$$\chi_H^2 = \sum_{i=1}^{57} \frac{[H^{obs}(z_i) - H^{th}(z_i)]^2}{\sigma(z_i)^2} \quad (27)$$

where  $H^{obs}$  and  $H^{th}$  are the observed and theoretical value of  $H$  and also  $\sigma(z_i)$  is the standard error in the measured value of  $H$ . The following plot shows nice fit to the  $H(z)$  datasets with suitable model parameter values compared with  $\Lambda$ CDM model. We have taken  $H_0 = 67.66 \text{ km/sec/Mpc}$  for our calculation.

The  $\chi^2$  function for the type Ia supernovae datasets is taken to be

$$\chi_{SN}^2 = \sum_{i=1}^{580} \frac{[\mu_{th}(\mu_0, z_i) - \mu_{obs}(z_i)]^2}{\sigma_{\mu(z_i)}^2}, \quad (28)$$

where  $\mu_{obs}$ ,  $\mu_{th}$ ,  $\sigma_{\mu(z_i)}$ , denotes the observed and theoretical distance modulus of the model, the standard error in the measurement of  $\mu(z)$  respectively. We fit free parameters of our model, comparing  $\mu_{obs}$  with theoretical values  $\mu_{th}$  of distance modulus. The distance model

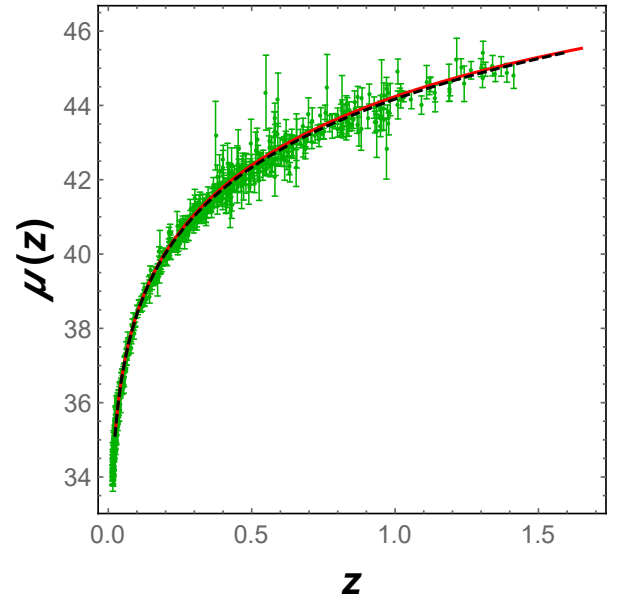


FIG. 11: The plot shows the 580 points of  $SN Ia$  datasets (Blue dots) with corresponding error bars along with the presented model (solid red line) which has a better fit to the  $SN Ia$  datasets for  $k_2 = 3$  and  $k_4 = -0.49$ .  $\Lambda$ CDM model is also shown in black dashed line for model comparison.

$\mu(z)$  is given by

$$\mu(z) = m = m' + 5 \text{Log} D_l(z) + \mu_0, \quad (29)$$

where  $D_l(z)$  and  $\mu_0$  are the luminosity distance and nuisance parameter respectively. Also  $m$  and  $m'$  serve as the apparent and absolute magnitudes of standard candle respectively. We calculate the  $\chi_{SN}^2$  function and the distance  $D_l(z)$  that measures differences between the  $SN Ia$  observational data and predictions of a model. The following plot shows nice fit to the  $SN Ia$  datasets with suitable model parameter values compared with  $\Lambda$ CDM model.

#### E. Estimation of model parameters with $H(z)$ , $SN Ia$ & BAO datasets

We can see, in the expression Eq.(21), we have only two model parameters  $k_2$  and  $k_4$ . Here, in this subsection, we shall find the constraints with the above discussed datasets i.e.  $H(z)$  and  $SN Ia$  together with one more external data, the Baryon Acoustic Oscillation (BAO) datasets for our analysis. The chi square value corresponding to BAO measurements is given by [65]

$$\chi_{BAO}^2 = B^T C^{-1} B, \quad (30)$$

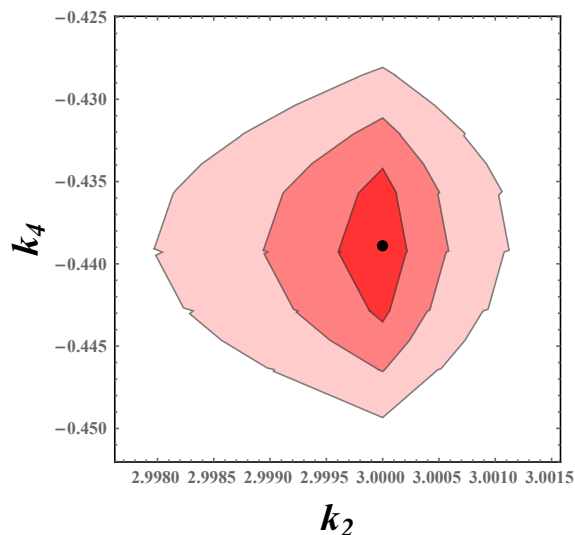


FIG. 12: The plot shows the contour plot for the model parameters  $k_2$  and  $k_4$  for independent  $H(z)$  datasets at  $1\text{-}\sigma$ ,  $2\text{-}\sigma$  and  $3\text{-}\sigma$  level in  $k_2$ - $k_4$  plane. The best estimated value is  $k_2 = 3$  and  $k_4 = -0.4389$ .

where the matrices  $B$ , inverse covariance matrix  $C^{-1}$  and the data details are discussed in the appendix.

With these three samples of datasets, we have found the likelihood contours for the model parameters  $k_2$  and  $k_4$  at  $1\text{-}\sigma$ ,  $2\text{-}\sigma$  and  $3\text{-}\sigma$  level and are plotted in the  $k_2$ - $k_4$  plane as shown in the figures. We have found constraints with independent  $H(z)$  datasets and combined  $H(z) + SNIa + BAO$  datasets. The best estimated values of the model parameters  $k_2$  and  $k_4$  are found to be  $k_2 = 3$ ,  $k_4 = -0.4389$  and  $k_2 = 3$ ,  $k_4 = -0.43374$  respectively for independent  $H(z)$  datasets and joint  $H(z) + SNIa + BAO$  datasets.

## V. CONCLUSION

In this article, we have studied a cosmological model in which we have discussed the phenomenon of cosmic acceleration without the need of dark energy but with a viscous fluid. With this effective viscosity EoS, the dynamical equation of the Hubble parameter is completely integrable and an exact solution for Einstein's field equation is obtained in modified  $f(R, T)$  gravity in the FLRW background. The effective EoS (pressure with additional bulk viscosity) describes the late-time acceleration of the Universe without introducing a cosmological constant or dark energy. We show that the matter described by an effective viscosity EoS can fit the observational data well, so the present effective viscosity model may be considered an alternative candidate to

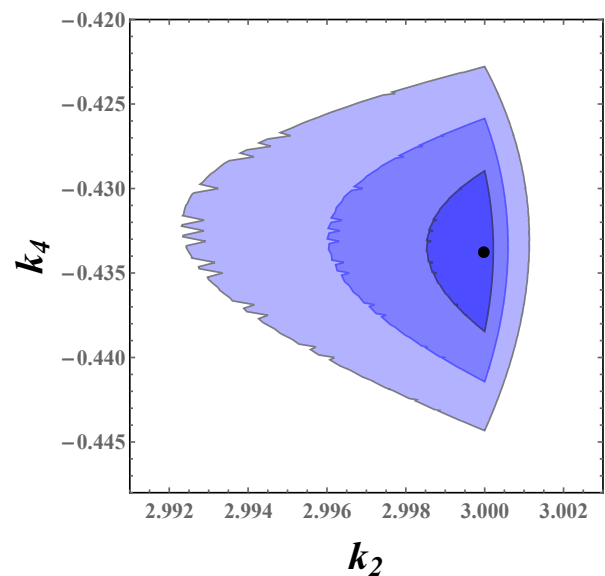


FIG. 13: The plot shows the contour plot for the model parameters  $k_2$  and  $k_4$  for combined  $H(z) + SNIa + BAO$  datasets at  $1\text{-}\sigma$ ,  $2\text{-}\sigma$  and  $3\text{-}\sigma$  level in  $k_2$ - $k_4$  plane. The best estimated value is  $k_2 = 3$  and  $k_4 = -0.43374$ .

explain the late-time accelerating expansion of the Universe.

The deceleration parameter shows a signature flip from early deceleration to present acceleration at  $z_t \approx 0.845815$  and  $z_t \approx 0.619797$  for  $k_4 = -0.43$  and  $k_4 = -0.49$  respectively with a negative value of the  $q_0 \approx -0.779046$  and  $q_0 \approx -0.684206$ , see Fig. 1. The evolution of the effective equation of state parameter  $\omega$  is shown in Fig. 4 showing the negative value of the  $\omega_0 \approx -0.888046$  for  $k_4 = -0.43$  and  $\omega_0 \approx -0.838394$  for  $k_4 = -0.49$  remains in the quintessence region (do not cross the phantom divide line  $\omega = -1$ ) approaching to  $-1$  in the infinite future leading to Einstein-de-Sitter model. It is also worth mentioning that the EoS parameter  $\omega$  shows a transition from positive pressure regime in the past to a negative pressure regime at present era implying that the incorporation of bulk viscous pressure term in the model plays a vital role for rendering a decelerating expansion in the past (suitable for structure formation) and an accelerated expansion at present. This can be seen in Fig. 4, which confirms from the standard cosmology that the latter regime may happen when  $\omega < -\frac{1}{3}$ . In the case, when  $\alpha = 0$  ( $\alpha$  is the coupling constant for modified gravity), the field equations (8) and (9) will reduce to general relativity and we can't get the same conditions where the pressure becomes negative throughout the evolution and the plot for  $w(z)$  remains in negative part (not shown). So, we can say that the coupling constant of modified gravity play a major

role in this context.

We have discussed some physical characteristics of the model and discussed the evolution of physical parameters together with the Energy Conditions. It is seen that NEC, DEC does not violate the model but SEC fails to satisfy, which produces a repulsive force and make the Universe to get jerk. The violation of SEC in Fig. 5 shows the viability of our model as mentioned in [50]. We have also discussed the velocity of sound favoring our model's consistency. Moreover, analysis of statefinder parameters and  $Om$  diagnostic also have been done and compared with the  $\Lambda$ CDM model. Finally, we have fitted our model with the updated 57 points of Hubble datasets and 580 points of Union 2.1 compilation Supernovae datasets compared with the  $\Lambda$ CDM model.

ECs have provided us with special insights into the deep structure for space and time in the cosmic space-time evolution processes. In the present model NEC and DEC validated whereas SEC is violated as per the requirement of cosmic acceleration (see Fig. 5). As we know the wormhole formation requires explicitly the null energy condition violation, which attracts us to further study the dark energy confrontation with the un-

common space time structure. We will publish the related work elsewhere soon. Further study can be done with this effective viscosity EoS in non-minimally coupled gravity.

### Acknowledgments

SA acknowledges CSIR, New Delhi, India for JRF. PKS acknowledges CSIR, New Delhi, India for financial support to carry out the Research project [No.03(1454)/19/EMR-II Dt.02/08/2019]. We are very much grateful to the honorable referees and the editor for illuminating suggestions that have significantly improved our work in terms of research quality as well as the presentation.

### Appendix

Details of  $H(z)$  datasets: The 57 points of Hubble parameter values  $H(z)$  with errors  $\sigma_H$  from differential age (31 points) method and BAO and other (26 points) methods are shown in the following table.

$z$	$H(z)$	$\sigma_H$	Ref.	$z$	$H(z)$	$\sigma_H$	Ref.
0.070	69	19.6	[66]	0.24	79.69	2.99	[67]
0.90	69	12	[68]	0.30	81.7	6.22	[69]
0.120	68.6	26.2	[66]	0.31	78.18	4.74	[70]
0.170	83	8	[68]	0.34	83.8	3.66	[67]
0.1791	75	4	[71]	0.35	82.7	9.1	[72]
0.1993	75	5	[71]	0.36	79.94	3.38	[70]
0.200	72.9	29.6	[73]	0.38	81.5	1.9	[74]
0.270	77	14	[68]	0.40	82.04	2.03	[70]
0.280	88.8	36.6	[73]	0.43	86.45	3.97	[67]
0.3519	83	14	[71]	0.44	82.6	7.8	[75]
0.3802	83	13.5	[76]	0.44	84.81	1.83	[70]
0.400	95	17	[68]	0.48	87.79	2.03	[70]
0.4004	77	10.2	[76]	0.51	90.4	1.9	[74]
0.4247	87.1	11.2	[76]	0.52	94.35	2.64	[70]
0.4497	92.8	12.9	[76]	0.56	93.34	2.3	[70]
0.470	89	34	[77]	0.57	87.6	7.8	[78]
0.4783	80.9	9	[76]	0.57	96.8	3.4	[79]
0.480	97	62	[66]	0.59	98.48	3.18	[70]
0.593	104	13	[71]	0.60	87.9	6.1	[75]
0.6797	92	8	[71]	0.61	97.3	2.1	[74]
0.7812	105	12	[71]	0.64	98.82	2.98	[70]
0.8754	125	17	[71]	0.73	97.3	7.0	[75]
0.880	90	40	[66]	2.30	224	8.6	[80]
0.900	117	23	[68]	2.33	224	8	[81]
1.037	154	20	[71]	2.34	222	8.5	[82]
1.300	168	17	[68]	2.36	226	9.3	[83]
1.363	160	33.6	[84]				
1.430	177	18	[68]				
1.530	140	14	[68]				
1.750	202	40	[68]				
1.965	186.5	50.4	[84]				

Details of BAO datasets: From very large scales, Baryon Acoustic Oscillation measures the structures in the universe. In this article, we have considered the sample of BAO distances measurements from surveys of SDSS(R) [85], 6dF Galaxy survey [86], BOSS CMASS [87] and WiggleZ [88]. So, the distance redshift ratio  $d_z$  is given as  $d_z = \frac{r_s(z_*)}{D_v(z)}$ , where  $r_s(z_*)$  is the co-moving sound horizon at the time photons decouple and  $z_*$  is the photon decoupling redshift. In accordance to Planck 2015 results [89],  $z_* = 1090$ . We have taken  $r_s(z_*)$  as considered in [90]. Also, dilation scale is read as  $D_v(z)$  and is given by  $D_v(z) = \left(\frac{d_B^2(z)z}{H(z)}\right)^{\frac{1}{3}}$ , where  $d_A(z)$  is the an-

gular diameter distance. The matrix  $B$  in the chi square formula of BAO datasets is given by  $d_B(z_*)/D_V(z_{BAO})$  and is calculated as

$$B = \begin{pmatrix} \frac{d_B(z_*)}{D_V(0.106)} - 30.95 \\ \frac{d_B(z_*)}{D_V(0.2)} - 17.55 \\ \frac{d_B(z_*)}{D_V(0.35)} - 10.11 \\ \frac{d_B(z_*)}{D_V(0.44)} - 8.44 \\ \frac{d_B(z_*)}{D_V(0.6)} - 6.69 \\ \frac{d_B(z_*)}{D_V(0.73)} - 5.45 \end{pmatrix},$$

and the inverse covariance matrix  $C^{-1}$  defined in [65] is

given by

$$C^{-1} = \begin{pmatrix} 0.48435 & -0.101383 & -0.164945 & -0.0305703 & -0.097874 & -0.106738 \\ -0.101383 & 3.2882 & -2.45497 & -0.0787898 & -0.252254 & -0.2751 \\ -0.164945 & -2.454987 & 9.55916 & -0.128187 & -0.410404 & -0.447574 \\ -0.0305703 & -0.0787898 & -0.128187 & 2.78728 & -2.75632 & 1.16437 \\ -0.097874 & -0.252254 & -0.410404 & -2.75632 & 14.9245 & -7.32441 \\ -0.106738 & -0.2751 & -0.447574 & 1.16437 & -7.32441 & 14.5022 \end{pmatrix}.$$

- [1] A. G. Riess et al., *Astron. J.* **116**, 1009 (1998).  
 [2] S. Perlmutter et al., *Astrophys. J.* **517**, 565 (1999).  
 [3] P. M. Garnavich et al., *Astrphys. J.* **493**, L53 (1998).  
 [4] S. Nojiri, S.D. Odintsov, *Phys. Rep.* **505**, 59 (2011).  
 [5] K. Bamba, S.D Odintsov, *Symmetry* **7**, 220 (2015).  
 [6] Z. Yousaf, M. Z. Bhatti, M. F. Malik, *Eur. Phys. J. Plus*, **134**, 470 (2019).  
 [7] Z. Yousaf et al. *Eur. Phys. J. C.*, **691**, 77 (2017).  
 [8] S. Nojiri, S.D. Odintsov, *Phys. Lett. B* **631**, 1 (2005).  
 [9] A. De Felice, S. Tsujikawa, *Phys. Rev. D* **80**, 063516 (2009).  
 [10] R. Myrzakulo, *Eur. Phys. J. C.* **72**, 2203 (2011).  
 [11] K. Bamba, *Eur. Phys. J. C.* **67**, 295 (2010).  
 [12] T. Harko, F.S.N. Lobo, S. Nojiri, S.D. Odintsov, *Phys. Rev. D* **84**, 024020 (2011).  
 [13] M. Z. Bhatti, Z. Yousaf, Zarnoor, *Gen. Relat. Gravit.*, **51**, 144 (2019).  
 [14] M. Z. Bhatti, Z. Yousaf, M. Yousaf, *Phys. Dark Universe*, **28**, 100501 (2020).  
 [15] P.H.R.S. Moraes, P.K. Sahoo, S.K.J. Pacif, *Gen. Relat. Gravit.*, **52**, 32 (2020).  
 [16] C. Eckart, *Phys. Rev.*, **58**, 919 (1940).  
 [17] H. Okumura, F. Yonezawa, *Physica A* **321** 207-219 (2003).  
 [18] I. Brevik, O. Gron, J. de Haro, S. D. Odintsov, E. N. Sardakis, *Int. J. Mod. Phys. D* **26**, 1730024 (2017).  
 [19] M. Sharif, Z. Yousaf, *JCAP* **06**, 019 (2014).  
 [20] S. D. Odintsov, Diego Saez-chillon Gomez, G.S. Sharov, *Phys. Rev. D* **101**, 044010 (2020).  
 [21] C. P. Singh, P. Kumar, *Eur. Phys. J. C.* **74**, 3070 (2014).  
 [22] W. Misner, *Astrophys. J.* **151**, 431 (1968).  
 [23] W. Israel, J.N. Vardalas, *Nuovo Cimento Lett.* **4**, 887 (1970).  
 [24] I. Wega, R. C. Falcao, R. Chanda, *Phys. Rev. D* **33**, 1839 (1986).  
 [25] T. Padmanabhan, S. Chitre, *Phys. Lett. A* **120**, 433 (1987).  
 [26] B. Cheng, *Phys. Lett. A* **160**, 329 (1991).  
 [27] G. C. Samanta, R. Myrzakulov, *Chin. J. Phys.* **55** 1044 (2017).  
 [28] S. Davood Sadatian, *EPL*, **126**, 30004 (2019).  
 [29] J. Ren, Xin-He Meng, *Phys. Lett B* **633**, 1 (2006).  
 [30] W. A. Hiscock, L. Lindblom, *Phys. Rev. D* **31**, 725 (1985).  
 [31] W. Israel, *Ann. Phys.* **100**, 310 (1976).  
 [32] W. Israel, J.M. Stewart, *Ann. Phys.* **118**, 341 (1979).  
 [33] A. Sasidharan, T. K. Mathew, *Eur. Phys. J.C.* **751**, 348 (2015).  
 [34] A. G. Riess et al., *Astrophys. J.* **607**, 665 (2004).  
 [35] D. J. Eisenstein et al., *Astrophys. J.* **633**, 560 (2005).  
 [36] S. B. Fisher, E. D. Carlson, *Phys. Rev. D* **100**, 064059 (2019).  
 [37] T. Harko, P. H.R.S. Moraes, *Phys. Rev. D* **101**, 108501 (2020).  
 [38] M. R. Setare, M. J. S Houndjo, *Can. J. Phys.* **91**(3), 260-267 (2013).  
 [39] M. Sharif, S. Rani, *Mod. Phys. Lett. A* **27**, 1350118 (2013).  
 [40] I. Brevik, *Entropy* **14**, 2302-2310 (2012).  
 [41] A. A. Mamon, S. Das, *Eur. Phys. J. C* **77**, 495 (2017).  
 [42] J. R. Garza et al., *Eur. Phys. J. C* **79**, 890 (2019).  
 [43] R. A. Knop et al., *Astrophys. J.* **598**, 102 (2003).  
 [44] E. E. O. Ishida et al. *Astropart. Phys.* **28** **6**, 547 (2008).  
 [45] J. V. Cunha, *Phys. Rev. D* **79**, 047301 (2009).  
 [46] N. Rani et al., *J. Cosmol. Astropart. Phys.* **1512**, 045 (2015).  
 [47] M. Visser, C. Barcelo, *COSMO-99*, 98 (2000).  
 [48] R. M. Wald, *General relativity* (University of Chicago Press, Chicago, 1984).  
 [49] S. W. Hawking, G. F. R. Ellis, *The Large Scale Structure of Space-Time* (Cambridge University Press, 1973).  
 [50] C. Barcelo, M. Visser, *Int. J. Mod. Phys. D* **11**, 1553 (2002).  
 [51] P.H.R.S. Moraes, P.K. Sahoo, *Eur. Phys. J. C.*, **77**, 480 (2017).  
 [52] M. Visser, *Phys. Rev. D* **56**, 7578 (1997).  
 [53] M.S. Linton et al., *J. Cosmol. Astropart. Phys.* **04**, 043 (2018).  
 [54] G. Ballesteros, J. Lesgourgues, *J. Cosmol. Astropart. Phys.* **10**, 014 (2010).  
 [55] V. Sahni, et al. *JETP Lett.* **77**, 201 (2003).  
 [56] M. Shahalam, Sasha Sami, Abhineet Agarwal, *Mon. Not. R. Astron. Soc.* **448**, 2948 (2015).

- [57] V. Sahni, A. Shafieloo, A. A. Starobinsky, *Phys. Rev. D* **78**, 103502 (2008).
- [58] C. Zunckel, C. Clarkson, *Phys. Rev. Lett.* **101**, 181301 (2008).
- [59] Jing-Zhao Qi et al., *Res. Astron. Astrophys.* **18**, 066 (2018).
- [60] A. Shafieloo, V. Sahni, A. A. Starobinsky, *Phys. Rev. D* **80**, 101301 (2009).
- [61] D. N. Spergel et al., *Astrophys. J. Suppl. Ser.* **170**, 377 (2007).
- [62] G. S. Sharov, V.O. Vasiliev, *Mathematical Modelling and Geometry* **6**, 1 (2018).
- [63] N. Suzuki et al., *Astrophys. J.* **746**, 85 (2012).
- [64] R. Nagpal, S. K. J. Pacif, J. K. Singh<sup>1</sup>, Kazuharu Bamba, A. Beesham, *Eur. Phys. J. C* **78**, 946 (2018).
- [65] R. Giotri et al., *J. Cosm. Astropart. Phys.*, **1203**, 027 (2012).
- [66] D. Stern et al., *J. Cosmol. Astropart. Phys.*, **02**, 008 (2010).
- [67] E. Gaztaaga, A. Cabre, L. Hui, *Mon. Not. Roy. Astron. Soc.*, **399**, 1663 (2009).
- [68] J. Simon, L. Verde, R. Jimenez, *Phys. Rev. D*, **71**, 123001 (2005).
- [69] A. Oka et al., *Mon. Not. Roy. Astron. Soc.*, **439**, 2515 (2014).
- [70] Y. Wang et al., *Mon. Not. Roy. Astron. Soc.* **469**, 3762 (2017).
- [71] M. Moresco et al., *J. Cosmol. Astropart. Phys.*, **08**, 006 (2012).
- [72] C. H. Chuang, Y. Wang, *Mon. Not. Roy. Astron. Soc.*, **435**, 255 (2013).
- [73] C. Zhang et al., *Research in Astron. and Astrop.*, **14**, 1221 (2014).
- [74] S. Alam et al., *Mon. Not. Roy. Astron. Soc.*, **470**, 2617 (2017).
- [75] C. Blake et al., *Mon. Not. Roy. Astron. Soc.*, **425**, 405 (2012).
- [76] M. Moresco et al., *J. Cosmol. Astropart. Phys.*, **05**, 014 (2016).
- [77] A.L. Ratsimbazafy et al., *Mon. Not. Roy. Astron. Soc.*, **467**, 3239 (2017).
- [78] C. H. Chuang et al. , *Mon. Not. Roy. Astron. Soc.*, **433**, 3559 (2013).
- [79] L. Anderson et al., *Mon. Not. Roy. Astron. Soc. ,* **441**, 24 (2014).
- [80] N. G. Busca et al., *Astron. Astrop.*, **552**, A96 (2013).
- [81] J. E. Bautista et al. *Astron. Astrophys.*, **603**, A12 (2017).
- [82] T. Delubac et al., *Astron. Astrophys. ,* **574**, A59 (2015).
- [83] A. Font-Ribera et al., *J. Cosmol. Astropart. Phys.*, **05**, 027 (2014).
- [84] M. Moresco, *Mon. Not. Roy. Astron. Soc.: Letters. ,* **450**, L16 (2015).
- [85] N. Padmanabhan et al., *Mon. Not. Roy. Astron. Soc.* **427**, 2132 (2012).
- [86] F. Beutler, C. Blake, M. Colless, D. H. Jones, L. Staveley-Smith, L. Campbell et al., *Mon. Not. Roy. Astron. Soc.* **416**, 3017 (2011).
- [87] BOSS collaboration, L. Anderson et al., *Mon. Not. Roy. Astron. Soc.* **441**, 24 (2014).
- [88] C. Blake et al., *Mon. Not. Roy. Astron. Soc.* **425**, 405 (2012).
- [89] P. A. R. Ade et al. [Planck Collaboration], *Astron. Astrophys.*, **571**, A16 (2014).
- [90] M. Vargas dos Santos, Ribamar R. R. Reis, *J. Cosm. Astropart. Phys.*, **1602**, 066 (2016).